# Nanocrystalline surface energy studied within the Gibbs thermodynamic framework

Mahach N. Magomedov *

*Institute for Geothermal Problems and Renewable Energy–Branch of Joint Institute for High Temperatures of Russian Academy Sciences, 39-a Shamil str., Makhachkala, Republic of Dagestan 367030, Russia*

(Received 6 June 2023; revised 8 September 2023; accepted 15 December 2023; published 5 January 2024)

In the equilibrium thermodynamics framework, expressions were obtained that determine the dependences of the specific surface energy $\sigma$ and surface pressure $P_{Sf}$ on the size ($N$) and shape of a freestanding nanocrystal at different pressure $P$ and temperature $T$. Based on these expressions, the behavior of the $\sigma(P, T, N)$ and $P_{Sf}(P, T, N)$ functions for fcc Au have been studied. The calculations performed for the macrocrystal showed good agreement with the experimental data. Calculations for a nanocrystal have shown that at $P = 0$, the $P_{Sf}(N)$ function lies in the negative region, i.e., the nanocrystal is stretched by surface pressure the more the higher of temperature, or the more the nanocrystal shape is deviated from an energy-optimal shape. With a decrease in $N$ at $P = 0$, the function $\sigma(N)$ decreases more noticeably the higher of temperature, or the more the nanocrystal shape deviates from an energy-optimal shape. Based on these results, it was shown that the increase in the $\sigma(N)$ function obtained in some articles with an isomorphic-isothermal decrease in $N$ does not correspond to the physical properties of nanoparticles. In these articles, the nanoparticle was compressed by surface pressure, which increased with an isomorphic-isothermal decrease of the $N$ value. This compression led to the corresponding growth of the $\sigma(N)$ function both with an isomorphic-isothermal decrease in size and with an isomeric (i.e., at $N = \text{const}$) increase in the nanoparticle temperature.

DOI: 10.1103/PhysRevB.109.035405

## I. INTRODUCTION

The value of the specific (per unit area) surface energy ($\sigma$) of a macrocrystal is one of the most important parameters determining its strength and adhesive properties. Therefore, much attention is paid to determining the $\sigma$ value. However, the experimental determination of the $\sigma$ value for the solid phase is a very labor-consuming procedure, implemented only at high temperatures [1,2]. At the same time, the accuracy of measuring the $\sigma$ value even at high temperatures is very approximate. Therefore, much attention is paid to the theoretical prediction of the $\sigma$ value for macrocrystals.

In recent years, in connection with the study of various nanocrystal properties, a large number of works have been devoted to the theoretical study of the size dependence of the $\sigma$ value. The relevance of this problem is due to the fact that it is the dependence of the $\sigma$ function on the nanocrystal size (or on the $N$—number of its atoms) that determines the size dependences of all the lattice properties of the nanocrystal. Unfortunately, due to the complexity of experimental measurement of the nanoparticle surface properties, there is currently no experimental dependence of the $\sigma$ function on the nanocrystal size in the literature. In view of this, despite the abundance of works devoted to methods of calculating the $\sigma(N)$ function, there is still no clear and unambiguous answer to the question: does the $\sigma(N)$ function decrease or increase with an isomorphic (i.e., with an unchanged shape) decrease in the nanocrystal atom number ($N$) at constant pressure $P$ and temperature $T$? In the modern literature (see reviews in Refs. [3–7]), there are theoretical articles that prove both the decrease (these are mainly analytical works) and the increase (this was obtained using computer simulation) of the $\sigma$ function with an isomorphic decrease in the nanoparticle size.

For example, in the article [5], a spherical core-shell model with radius ($R$) was studied by the method "a combination of atomic modeling and continuum mechanics." Calculations carried out in Ref. [5] for a gold nanocrystal at $T = 0$ K showed that the $\sigma(R)$ function increases with an isomorphic decrease in the radius of the nanocrystal.

Another example can be given. In the article [6], Amara and co-authors investigated the change in the $\sigma$ function with an isomorphic change in the size and temperature of metal nanoparticles, both in the solid and the liquid state. They used the $N$-body interatomic potentials and the Monte Carlo method, and performed analytical calculations too. A solid nanocrystal was studied at a temperature of $T = 5$ K, and a liquid nanodrop at $T = 1500$ K. The authors [6] obtained that for a freestanding nanoparticle the $\sigma$ function increases with a decrease in the nanoparticle size in both solid ($\sigma_s$) and liquid ($\sigma_l$) phases.

The works that obtained an increase in the $\sigma$ function with isomorphic-isothermal reduction of the nanoparticle size exploit the fact that there is no experimental dependence of the $\sigma$ function on the nanoparticle size in the literature. However, although there is no experimental dependence of $\sigma(N)$ in the literature, the function $\sigma(N)$ has a certain physical meaning, and it is related to other properties of the nanoparticle that can be measured, such as the melting point. Therefore, the results of the works that prove the increase of the $\sigma$ function

*mahmag4@mail.ru

 

with an isomorphic-isothermal decrease in the nanoparticle size, do not correspond to the physical properties of real metal nanoparticles for the following reasons.

(1) Since Tolman's time, it has been accepted that with a decrease in the size of the nanodrop, the $\sigma_l$ function decreases [8]. According to Tolman, for a single-component liquid, the dependence of the $\sigma_l$ function on the radius ($r$) of a spherical nanodrop can be represented as follows [8,9]:

$$\sigma_l(r) = \frac{\sigma_l(\infty)}{1+2\frac{\delta}{r}} \cong \sigma_l(\infty)\left(1-2\frac{\delta}{r}\right).$$

Here $\sigma_l(\infty)$ is the surface energy of the macrodrop and $\delta = r_e – r$ is the difference between the equimolar radius and the nanodrop radius; $\delta$ is also called Tolman length.

Various expressions have been proposed to calculate the $\delta$ value. For example, the following relations were obtained for relatively large droplets:

$$\delta = d_a \text{ [10]}, 0.725d_a \text{ [11]}, r_o/3 \text{ [12]}, 0.376r_o \text{ [13]},$$

where $d_a$ is the atomic diameter and $r_o$ is the coordinate of the minimum of the Mie–Lenard-Jones interatomic potential with powers of 6–12. In addition, in Ref. [9] it was obtained that $\delta = \alpha_m/4$, where $\alpha_m$ is the parameter determining the size dependence of the melting temperature ($T_m$) for a spherical nanocrystal at atmospheric pressure ($P = 1$ atm):

$$T_m(r) = T_m(\infty)\left(1-\frac{\alpha_m}{2r}\right) = T_m(\infty)\left(1-\frac{2\delta}{r}\right).$$

In Ref. [9], the $\delta$ values were calculated for 49 solid metals. The $\delta$ values for liquid inert gases were calculated in Ref. [13]. All these results show that $\delta > 0$. This contradicts the dependencies obtained in the works, in which the $\sigma$ function increases with isomorphic-isothermal decrease of the nanoparticle size.

(2) In [6, Fig. 2(a)] it was obtained that when the radius of the fcc-Cu crystal decreases from macroscopic ($r = \infty$) to $r = 5$ Å, the $\sigma_s$ value increases almost twofold: from 1.1–1.2 to 1.9–2 J/m$^2$. For the fcc-Cu macrocrystal, the experimental specific surface energy value is equal to $\sigma_s(\infty) = 2 \pm 0.1$ J/m$^2$ [14]. However, if we adopt the result from [6, Fig. 2(a)] [i.e., $\sigma_s(r = 5\text{ Å})/\sigma_s(r = \infty) = 2/1.2 = 1.67$ ], then the copper nanoparticle with a radius of 5 Å will have a specific surface energy equal to $\sigma_s(r = \infty) = 1.67 \times (2 \pm 0.1\text{ J/m}^2) = 3.34 \pm 0.167$ J/m$^2$. According to Ref. [14], the experimental values for the Mo and W macrocrystals are equal to $\sigma_s(\infty) = 2.91 – 3.00$ J/m$^2$ (for Mo) and $3.265 – 3.68$ J/m$^2$ (for W). Thus, according to the results from Ref. [6], for the fcc-Cu nanocrystal with radius $r = 5$ Å, the $\sigma$ value should reach values corresponding to the specific surface energies of the macrocrystals Mo or W.

(3) When studying the Cu nanodrop in [6, Fig. 2(a)], an increase in the $\sigma_l$ function from $\sigma_l(r = \infty) = 1.2$ J/m$^2$ to $\sigma_l(r = 5\text{ Å}) = 2.3$ J/m$^2$ was obtained. This result is surprising too, because according to the experimental data for macrosystems, the following relationship is observed between the surface energies of the solid and liquid phases: $\sigma_s/\sigma_l = 1.09 – 1.33$ [1,15]. Herewith, as was shown in Ref. [16], when the atom number in the nanosystem decreases, the $\sigma_s/\sigma_l$ function decreases to 1. Therefore, if the $\sigma_l$ function increases to the macrocrystal value as the nanodrop size decreases, then this nanodrop would have to crystallize. Moreover, in [6, Figs. 2(b) and 7(a)] the value of $\sigma_l(T = 1500\text{ K})$ turned out to be greater than $\sigma_s(T = 5\text{ K})$ for both the macro- and the nanosystem. This result clearly contradicts the physics of nanoparticles.

(4) As for the experimental study of the size dependence of the specific surface energy, such experiments were carried out for the liquid phase in Refs. [17,18]. In these experiments, it was found that the $\sigma_l(r)$ function decreases with a decrease in the nanodrop size. It is also possible to point to the results from Ref. [19], where a system of submillimeter grains that acoustically levitate in the air was studied. These levitating grains self-assemble into a monolayer of particles, forming mesoscopic granular rafts whose behavior is similar to a drop of liquid. In Ref. [19] it was found that the effective surface tension and elastic modulus of the raft decrease with a decrease in the size of the raft.

All these inconsistencies caused us to doubt the correctness of surface energy calculation methods, which were used in theoretical works, where an increase of the $\sigma$ function was obtained with an isomorphic-isothermal decrease of the nanoparticle size. In accordance with this, the question arises—why, when using computer simulation (in Refs. [5,6] and in other works), an increase in the $\sigma$ value has been obtained with an isomorphic-isothermal decrease in the nanoparticle size? How does one obtain the correct size dependence of the function $\sigma(N)$? How will this size dependence $\sigma(N)$ change at different temperatures and pressures in a nanocrystal? In this paper, we will try to answer these questions within the framework of equilibrium and reversible thermodynamics, using the analytical method developed by us for calculating the $\sigma(T, P, N)$ function.

## II. CALCULATING METHOD

Consider a condensed nanosystem of $N$ identical atoms, which is bounded by a surface. To apply the methods of equilibrium and reversible thermodynamics to such a system, we must postulate that the system surface is a geometric Gibbs surface that has no thickness. If we assume that the surface layer has a thickness ($\delta$), then this will introduce uncertainty into the calculation of the system volume, and questions will arise both about the surface layer thickness and about the change in the thermodynamic properties of the substance inside this layer. To get around these problems, Gibbs introduced a "dividing surface" instead of a real interphase boundary [20, Ch. 15; 21, Ch. 19], to which all surface characteristics belong. With this, the following equilibrium conditions must be observed at each point ($x$) of such a nanosystem: thermal [$T(x) = \text{const}$], mechanical [$P(x) = \text{const}$], and chemical [$\mu_g(x) = \text{const}$] equilibrium conditions.

The change in the Helmholtz free energy ($F_H$) of such a system with variations in temperature, volume ($V$), atoms number, and surface area ($\Sigma$) in the framework of equilibrium and reversible thermodynamics is usually represented as

follows [20, Ch. 2; 21, Ch. 6]:

$$\begin{aligned} dF_H &= \left(\frac{\partial F_H}{\partial T}\right)_{N,V,\Sigma} dT + \left(\frac{\partial F_H}{\partial V}\right)_{N,T,\Sigma} dV \\ &+ \left(\frac{\partial F_H}{\partial N}\right)_{T,V,\Sigma} dN + \left(\frac{\partial F_H}{\partial \Sigma}\right)_{N,V,T} d\Sigma \\ &= -\,SdT - PdV + \mu_g dN + \sigma d\Sigma, \end{aligned} \tag{1}$$

where $S$ is the entropy and $\mu_g$ is the chemical potential.

From Eq. (1) it is easy to see that the specific surface energy is

$$\sigma(T, v, N) = \left(\frac{\partial F_H}{\partial \Sigma}\right)_{T,v=V/N,N} = \left(\frac{\partial f_H}{\partial(\Sigma/N)}\right)_{T,v,N}. \tag{2}$$

Herewith, the change in the specific surface $\Sigma/N$ must occur in a reversible way, i.e., without irreversible destruction of the system, i.e., without violating the axioms of equilibrium and reversible thermodynamics.

However, at $N = \text{const}$, it is impossible to isomorphically change the surface area without changing the volume, because at a constant of the nanocrystal shape, these values are related by the ratio $\sum \sim V^{2/3}$. Therefore, as was stated in [22,23], at $\Sigma/N \neq 0$, the $\sigma$ function can be determined only by isochoric-isothermal reversible deformation of the nanosystem shape, i.e., by means of the expression

$$\begin{aligned} \sigma(T, v, N, f) &= \left(\frac{\partial f_H}{\partial(\Sigma/N)}\right)_{T,N,v} \\ &= \left(\frac{\partial f_H}{\partial f}\right)_{T,N,v} \Bigg/ \left(\frac{\partial(\Sigma/N)}{\partial f}\right)_{T,N,v}, \end{aligned} \tag{3}$$

where $v = V/N$, $f$ is a parameter that determines the shape of a system with a finite value of the number of atoms $N$, and which is bounded by a surface area $\Sigma$.

It can be seen from Eq. (1) that the pressure in the nanosystem should be calculated by the expression

$$P(T, v, N) = -\left(\frac{\partial f_H}{\partial v}\right)_{T,N,\Sigma}. \tag{4}$$

However, at constant values of $T$, $N$, and $\Sigma$, it is impossible to change the specific volume of the nanosystem. To get around this problem, it is necessary to assume that the system surface is a geometric Gibbs surface, and to represent the specific free energy as the sum of the volume and surface contributions as follows [20, Ch. 15]:

$$f_H(T, v, N, f) = f_{H\,\text{in}}(T, v) + \sigma(T, c, N, f)\frac{\Sigma}{N}. \tag{5}$$

Here the specific Helmholtz free energy for the nanosystem volume is

$$f_{H\,\text{in}}(T, v) = \lim_{N\to\infty}\left[\frac{F_H(T, v, N, f)}{N}\right]_{v=\text{const}}, \tag{6}$$

where $c = (6k_p v/\pi)^{1/3}$ is the average (over the nanosystem volume) distance between the centers of the nearest atoms and $k_p$ is the packing coefficient of the structure from $N$ atoms.

Then from Eq. (5) for the pressure in the nanosystem we obtain the expression

$$P(T, v, N, f) = -\left(\frac{\partial f_H}{\partial v}\right)_{T,N} = P_{\text{in}}(T, v) - P_{Sf}(T, c, N, f). \tag{7}$$

Here, $P_{\text{in}}$ is the "volume" pressure, i.e., the pressure determined without taking into account the surface term in Eqs. (1) and (5) as follows:

$$P_{\text{in}}(T, v) = -\lim_{N\to\infty}\left[\frac{\partial f_{H\,\text{in}}}{\partial v}\right]_{T,N}. \tag{8}$$

The $P_{Sf}$ function is the surface pressure, which is equal to [23,24]

$$P_{Sf}(T, c, N, f) = \left[\frac{\partial(\sigma\Sigma/N)}{\partial v}\right]_{T,N} = P_{Ls}(1 - \Delta_p). \tag{9}$$

The first factor in Eq. (9) is the Laplace pressure, which is determined by the change in surface area with the change in the nanosystem volume as follows:

$$\begin{aligned} P_{Ls}(T, v, N, f) &= \sigma\left[\frac{\partial(\Sigma/N)}{\partial v}\right]_{T,N} \\ &= \sigma\left(\frac{\Sigma/N}{v}\right)\left[\frac{\partial \ln(\Sigma/N)}{\partial \ln(v)}\right]_{T,N}. \end{aligned} \tag{10}$$

The expression for the $\Delta_p$ function from Eq. (9) has the form

$$\Delta_p = -\left[\frac{\partial \ln(\sigma)}{\partial \ln(\Sigma/N)}\right]_{T,N} = -\left[\frac{\partial \ln(\sigma)}{\partial \ln(\Sigma)}\right]_{T,N}. \tag{11}$$

For the liquid phase, the following is performed: $(\partial\sigma/\partial\Sigma)_{T,N} = 0$. This is due to the dynamic nature of the liquid state, where a large proportion of atoms are in a delocalized state. Isothermal stretching of the liquid phase surface area causes an influx of new atoms from the volume to its surface. If the influx of atoms to the surface occurs at a rate sufficient for the surface density of atoms to remain unchanged, then the $\sigma$ value for the liquid phase will not change with the growth in $\Sigma$, and therefore the $\Delta_p$ value will be zero. That is why the condition $\Delta_p = 0$, as was shown in Ref. [25], can be used as a "surface melting" criterion for a system with a geometric Gibbs surface. However, for the solid phase it is impossible to assume that $\Delta_p = 0$. Nagaev first pointed this out [26].

If the crystal structure (characterized by the packing coefficient $k_p$) and the surface shape (characterized by the shape parameter $f$) do not change with an isothermal change in the specific volume, then the functions $P_{Ls}$ and $\Delta_p$ from (10) and (11) will take the forms

$$P_{Ls} = \sigma\left(\frac{\Sigma/N}{v}\right)\left[\frac{\partial \ln(\Sigma/N)}{\partial \ln(v)}\right]_{T,N,k_p,f} = \frac{2}{3}\sigma\left(\frac{\Sigma/N}{v}\right), \tag{12}$$

$$\Delta_p = -\left[\frac{\partial \ln(\sigma)}{\partial \ln(\Sigma)}\right]_{T,N} = -\frac{1}{2}\left[\frac{\partial \ln(\sigma)}{\partial \ln(c)}\right]_{T,N,k_p,f}. \tag{13}$$

Thus, for further calculations, it is necessary, using Eq. (3), to determine the $\sigma(T, c, N, f)$ function. To do this, it is necessary to adopt a certain geometric model of a nanocrystal with a variable surface shape.

As in Refs. [22–25], we assume that a nanocrystal with a free Gibbs surface has the shape of a rectangular parallelepiped with a square base and faces of the (100) type. Limiting the system by the surface leads to the bonds breaking at the boundary. Therefore, if the "only nearest neighbors interaction" approximation is used, then instead of the first coordination number ($k_n$), it is necessary to take the $\langle k_n \rangle$ function, which is the average (over the entire nanosystem) value of the first coordination number. The $\langle k_n \rangle$ function depends on both the size ($N$) and the nanosystem shape ($f$) according to the formula [22–24]

$$k_n^* = \frac{\langle k_n(N,f)\rangle}{k_n(\infty)} = 1 - Z_s(f)\left(\frac{\alpha^2}{N}\right)^{1/3},$$
$$Z_s(f) = \frac{1+2f}{3f^{2/3}}. \tag{14}$$

Here, $k_n(\infty) = k_n(N=\infty)$ is the coordination number for the macrocrystal, $\alpha = \pi/(6k_p)$ is the structure parameter, and $f = N_{ps}/N_{po}$ is the shape parameter, which is defined by the ratio of the number $N_{ps}$ of atoms on the side edge to the number $N_{po}$ of atoms on the base edge. It is obvious that $f > 1$ for a rodlike shape, $f = 1$ for a cube, and $f < 1$ for a platelike shape. With this, we assume that the structure of the nanosystem remains unchanged: $k_p = \text{const}$. This model of a nanocrystal in the form of a rectangular parallelepiped, whose shape can be varied by the shape parameter $f$, was called the RP model.

The shape function $Z_s(f)$ included in Eq. (14) reaches a minimum equal to unity at $f = 1$, i.e., for a system that has the cube shape. For platelike ($f < 1$) or rodlike ($f > 1$) shapes, the $Z_s(f)$ value is larger than unity: $Z_s(f \neq 1) > 1$. Therefore, the $k_n(f)^*$ function for any $N$ value has a maximum at $f = 1$, i.e., for the energy-optimal cubic shape of a rectangular parallelepiped.

The surface volume and area for the RP model are [22–24]

$$V = N_{po}^3 f c^3 = N\alpha c^3,$$
$$\Sigma = 6c^2(N\alpha^2)^{2/3} Z_s(f).$$

It is easy to see that the nanocrystal volume does not depend on the system shape, i.e., on the $f$ value.

Let us represent the paired interatomic interaction in the form of the Mie–Lennard-Jones potential, which has the following expression [21]:

$$\varphi(r) = \frac{D}{(b-a)}\left[a\left(\frac{r_o}{r}\right)^b - b\left(\frac{r_o}{r}\right)^a\right], \tag{15}$$

where $D$ and $r_o$ are the depth and potential minimum coordinate and $b$ and $a$ are the numerical parameters such that $b > a > 1$.

Using the only nearest neighbors interaction approximation, in the framework of the RP model, the expressions for the specific surface energy of the nanocrystal face (100) and for the surface pressure were obtained as follows [27]:

$$\sigma(N,f) = -\frac{k_n(\infty) D R^2}{12\alpha^{2/3} r_o^2} L_E(N,f), \tag{16}$$
$$P_{Sf} = \frac{4\alpha^{1/3} Z_s(f)}{N^{1/3} c}\sigma(1-\Delta_p). \tag{17}$$

Here, $R = r_o/c$ is the relative linear density of the crystal; the Laplace pressure and the introduced functions have the following forms [27]:

$$P_{Ls} = \frac{4\alpha^{1/3} Z_s(f)}{N^{1/3} c}\sigma = 4\frac{(1-k_n^*)}{\alpha^{1/3} c}\sigma, \tag{18}$$

$$L_E(N,f) = U(R) + 3H_w(N,T),$$
$$\Delta_p = -\frac{1}{2}\left[\frac{\partial \ln(\sigma)}{\partial \ln(c)}\right]_{T,N,k_p,f}$$
$$= 1 + \frac{1}{2L_E(N,f)} \times \left\{U'(R) - 9\left[q - \gamma t_y\left(\frac{\Theta_E}{T}\right)\right]H_w(N,T)\right\}, \tag{19}$$

$$H_w(N,T) = \frac{6\,\gamma(N,f)}{(b+2)}\left[\frac{k_B\Theta_E(N,f)}{D\,k_n(N,f)}\right]E_w\left(\frac{\Theta_E}{T}\right),$$
$$U(R) = \frac{aR^b - bR^a}{b-a},$$
$$U'(R) = R\left[\frac{\partial U(R)}{\partial R}\right] = \frac{ab(R^b - R^a)}{b-a},$$
$$E_w(y) = 0.5 + \frac{1}{[\exp(y)-1]},$$
$$t_y(y) = 1 - \frac{2y\exp(y)}{[\exp(2y)-1]}. \tag{20}$$

Here, $k_B$ is the Boltzmann constant. Expressions for the Einstein temperature ($\Theta_E$), and the first $[\gamma = -(\partial \ln \Theta_E/\partial \ln v)_T]$ and second $[q = (\partial \ln \gamma/\partial \ln v)_T]$ Grüneisen parameters have been presented in Ref. [27].

It is obvious that in the "thermodynamic limit" (i.e., when $N \to \infty$ and $V \to \infty$ at $v = V/N = \text{const}$), the functions $P_{Ls}$ from Eq. (18) and $P_{Sf}$ from Eq. (17) disappear, for in this case $k_n^*(N \to \infty) \to 1$, and the expressions from (16), (19), and (20) are converted to formulas for the macrocrystal.

The use of this RP model made it possible to study the dependence of the specific surface energy on both the size and the nanocrystal shape at various $P$-$T$ conditions in Refs. [27–32]. Details of the method application and its results can be found in these articles.

## III. CALCULATION RESULTS

To calculate the dependence of the surface energy on the nanocrystal size, we choose gold [Au; $m(\text{Au}) = 196.967$ amu]. Gold has a fcc structure [$k_n = 12$, $k_p = 0.7405$, $\alpha = \pi/(6k_p) = 0.707\,09$] and does not experience polymorphic phase transitions up to 220 GPa [33].

For fcc Au, the parameters of the paired interatomic potential (15) were determined by our self-consistent method in Ref. [31], and they have the following values:

$$r_o = 2.87 \times 10^{-10}\ \text{m}, \quad \frac{D}{k_B} = 7446.04\ \text{K},$$
$$b = 15.75, \quad a = 2.79. \tag{21}$$

There are statements in the literature that the pairwise four-parametric Mie–Lennard-Jones potential (15) in

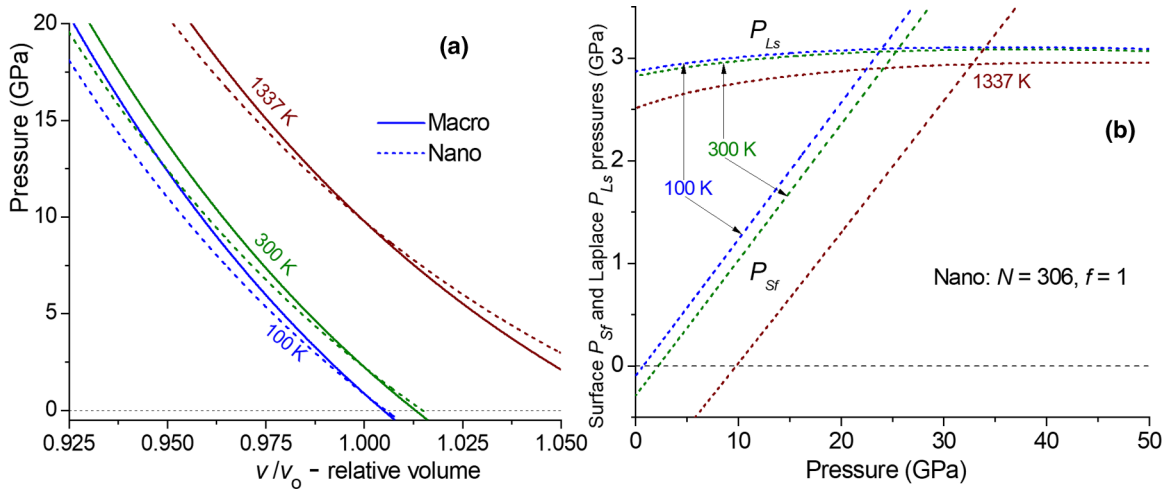


FIG. 1. (a) Isomorphic-isomeric dependences of pressure on normalized volume for fcc Au. Solid lines were obtained for a macrocrystal, and dashed lines were obtained for a nanocrystal. Isotherms are shown (bottom to top): $T = 100$, 300, 1337 K. (b) Isomorphic-isomeric baric dependences of Laplace pressure ($P_{Ls}$) and surface pressure ($P_{Sf}$) for a nanocrystal of 306 atoms. Isotherms are shown (top to bottom): $T = 100$, 300, 1337 K.

a methodological sense is inferior to, e.g., potentials based on the tight-binding approximation, which have a quantum-mechanical foundation. However, as we have shown in Refs. [27,34,35], the potential (15) with parameters from (21) allows us to obtain good agreement with experimental data for all thermodynamic properties and baric dependence of the melting temperature of the fcc-Au macrocrystal. Therefore, in this paper, we have studied the change in the state equation and surface energy during the transition from macrocrystal to nanocrystal based on the potential parameters (21).

A cubic nanocrystal of $N = f\ N_{\rm po}^3/\alpha = 306$ atoms (i.e., with $N_{\rm po} = 6$, $f = 1$, $k_n^* = 0.8822$) with a free geometric Gibbs surface was taken for the calculations. Figure 1(a) shows isomorphic-isomeric (i.e., at constants of $f$ and $N$) pressure dependences ($P$, in GPa) on the normalized volume [$v/v_{\rm o} = (c/r_{\rm o})^3 = R^{-3}$] for the macro- and nanocrystal of fcc Au. Solid lines were obtained for a macrocrystal (i.e., at $N = \infty$) and dashed lines were obtained for a cubic nanocrystal of $N = 06$ atoms. A decrease in pressure growth during the transition from macro- to nanocrystal indicates a decrease in the elastic modulus: $B_T = -v(\partial P/\partial v)_T$, with a decrease in the nanocrystal size. Other authors also obtained a decrease in the $B_T$ function with a decrease in the nanocrystal size theoretically and experimentally in Refs. [36–40].

It can be seen from Fig. 1 that at a certain value of relative volume $(v/v_{\rm o})_0$, the $P(v/v_{\rm o})$ dependences for a nanocrystal and a macrocrystal intersect. Thus, at $(v/v_{\rm o})_0$, the surface pressure $[P_{Sf}(v) = P(v)_{\rm Macro} – P(v)_{\rm Nano}]$ becomes zero: $P_{Sf}(v/v_{\rm o})_0 = 0$. At $v/v_{\rm o} < (v/v_{\rm o})_0$, the surface pressure compresses the nanocrystal ($P_{Sf} > 0$), and at $v/v_{\rm o} > (v/v_{\rm o})_0$, the surface pressure stretches the nanocrystal ($P_{Sf} < 0$). The $(v/v_{\rm o})_0$ value decreases with both an isomorphic-isomeric ($f, N = {\rm const}$) increase in the temperature and an isomorphic-isothermal ($f, T = {\rm const}$) decrease in $N$ or upon the isomeric-isothermal ($N$,$T = {\rm const}$) deviation of a nanocrystal shape from the most energy-optimal shape (for the RP model it is a cube). It also follows from Fig. 1 that the pressure in the nanocrystal passes through zero at a $v/v_{\rm o}$ value greater than for the macrocrystal. Figure 1(b) shows that the surface pressure increases with the pressure more noticeably than the Laplace pressure. If at low pressures $P_{Ls} > P_{Sf}$ is fulfilled, then at high pressures this inequality is reversed.

Figure 2 shows the calculated baric (a) and temperature (b) isomorphic-isomeric dependences of the specific surface energy ($\sigma$, in J/m$^2$ = N/m) for the face (100) in fcc Au. Solid lines were obtained for a macrocrystal (i.e., at $N = \infty$) and dashed lines were obtained for a cubic nanocrystal of $N = 306$ atoms. As was shown in Ref. [34], our calculations of the $\sigma(100)$ value for the fcc-Au macrocrystal are in good agreement with experimental and theoretical estimates by other authors. The experimental and theoretical (in parentheses) $\sigma(100)$ values for the fcc-Au macrocrystal presented in the literature are equal:

$$\sigma(100)/[{\rm J/m^2}] = 1.54\,(T = 0\,{\rm K})–1.333(T_m = 1337\,{\rm K})\ [1],$$

$$[1.363\,(T = 0\,{\rm K})]\ [4],\ [1.359\,(T = 0\,{\rm K})]\ [14].$$

Figure 2 shows that as the temperature decreases, there is a pressure region where the specific surface energy of the nanocrystal becomes greater than that of the macrocrystal, i.e., $\sigma(N) > \sigma(\infty)$. As was shown in Refs. [27,29–32], this effect is associated with the compression of the nanocrystal by surface pressure at low temperatures. As was shown in Refs. [23,24], the surface pressure in a nanocrystal consists of two competing forces:

(i) The resultant component of the attraction forces of the surface atom from the surrounding neighboring atoms. This force (maximum for the atoms on the edges, and especially at the vertices of the parallelepiped) tends to pull the surface atom inside the nanocrystal. This force compresses the nanocrystal the stronger the smaller the value of the "size argument" $k_n^*$.

(ii) The force arising from vibrations ("zero" at $T = 0$ K, or "thermal" at $T > 0$ K) of atoms. This force tends to push

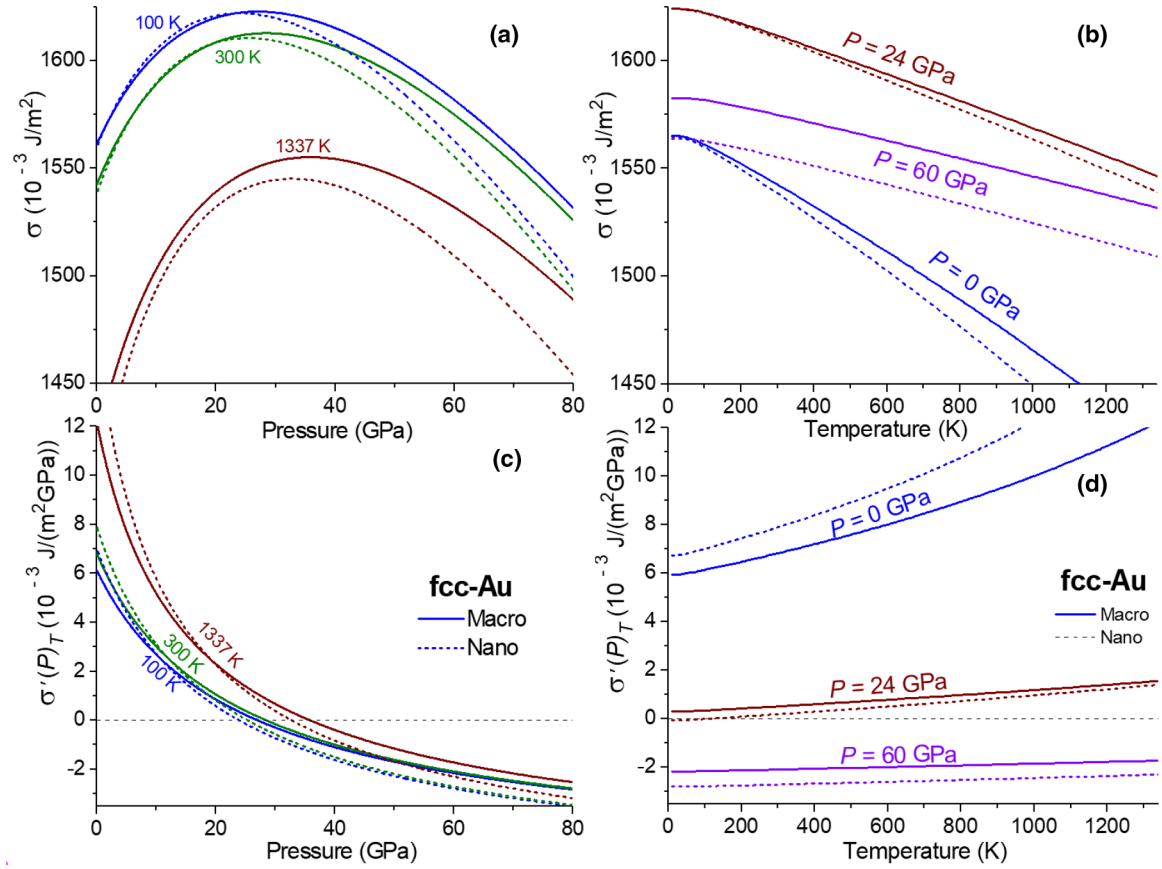


FIG. 2. The upper graphs show the baric (a) and temperature (b) isomorphic-isomeric dependences of the specific surface energy $\sigma(100)$. The lower graphs show the baric (c) and temperature (d) isomorphic-isomeric dependences of the isothermal derivative of the $\sigma(100)$ function on pressure: $\sigma'(P) = (\partial\sigma/\partial P)_T$. The graphs on the left from top to bottom show the isotherms: $T = 100$, 300, 1337 K. The graphs on the right show isobars: $P = 0$, 60, 24 GPa. Solid lines were obtained for a macrocrystal, and dashed lines were obtained for a nanocrystal.

the surface atom out of the nanocrystal, and it is this force that stretches the nanocrystal. Moreover, the energy and pressure caused by the vibrations of atoms increase with temperature.

At low temperatures, for "nonquantum" crystals (i.e., for which the "zero vibrations" energy of atoms is much less than the interatomic interaction energy), the first force prevails. However, with an increase in temperature, the second force grows, and at the "temperature of zero surface pressure," these forces balance each other [24].

As can be clearly seen from Figs. 2(a) and 2(b), at $P = 0$, the $\sigma(N)$ function decreases more noticeably with decreasing $N$ the higher the temperature. In the region of $P < 20$ GPa, the $\sigma$ function increases under isothermal compression for both macro- and nanocrystal of 306 atoms.

The lower graphs of Fig. 2 show the baric [graph (c)] and temperature (d) dependences of the derivative of specific surface energy on pressure: $\sigma'(P) = (\partial\sigma/\partial P)_T$ in $10^{-3}$ J/(m$^2$GPa). Solid lines were obtained for a macrocrystal (i.e., at $N = \infty$) and dashed lines were obtained for a cubic nanocrystal of $N = 306$ atoms. As can be seen from Figs. 2(c) and 2(d), there are points on the isotherms at a certain pressure ($P_\sigma$) where the $\sigma'(P)_T$ dependencies for macro- and nanocrystal intersect: $\sigma'(P_\sigma)_{T,\infty}$–$\sigma'(P_\sigma)_{T,N} = 0$. At these points, the size dependence of the function $\sigma'(P)_T$ changes. When $P < P_\sigma$, the function $\sigma'(P)_T$ increases with decreasing $N$, and when $P > P_\sigma$, the function $\sigma'(P)_T$ decreases at the isothermal-isobaric decreasing of $N$ value.

As can be seen from Figs. 2(c) and 2(d), the value of $\sigma'(P)_T$ increases with the isomer-isobaric increase in temperature. With this, the temperature growth of the function $\sigma'(P)_T$ slows down with increasing pressure.

Table I shows the properties of fcc Au calculated for three temperatures, indicated in the first column. The second, third, and fourth columns show the values of the normalized volume: $v/v_o = (c/r_o)^3$, the specific surface energy of the face (100), the value of the function $\Delta_p(N) = 1–(P_{Sf}/P_{Ls})$, both for the macrocrystal at $P_{\text{Macro}} = 0$ (first row), and for a cubic nanocrystal of 306 atoms at $P_{\text{Nano}} = 0$ (second row). The fifth column shows the values of the $P_{\text{Nano}}$ pressure at which the nanocrystal is located if $P_{\text{Macro}} = 0$ (top row), and the $P_{\text{Macro}}$ pressure at which the macrocrystal is located if $P_{\text{Nano}} = 0$ (bottom row) [see Fig. 1(a)]. The two right columns show the maximum point coordinates of the $\sigma(P)$ function in Fig. 2(a): for each temperature, the first row shows the data for a macrocrystal, and the second row shows the data for a cubic nanocrystal of 306 atoms.

From Eq. (16), it is possible to obtain expressions for isochoric and isobaric derivatives of the $\sigma(N, f)$ function with

TABLE I. Values of fcc-Au surface properties. For each temperature, the first row shows the results calculated for a macrocrystal, and the second row shows the results for a cubic nanocrystal of 306 atoms.

| $T$, K | $v/v_o$ | $\sigma(100)$ ($10^{-3}$ J/m$^2$) | $\Delta_p$ | $P_{\text{Nano}}$ (GPa)<br>$P_{\text{Macro}}$ (GPa) | $\sigma_{\max}$ ($10^{-3}$ J/m$^2$) | $P_{\max}$ (GPa) |
|---|---|---|---|---|---|---|
| 100 | 1.00487 | 1561.19 | 1.0299 | 0.090 | 1623 | 27.0 |
| | 1.00547 | 1559.84 | 1.0342 | –0.101 | 1622 | 23.9 |
| 300 | 1.01302 | 1542.47 | 1.0903 | 0.255 | 1613 | 28.6 |
| | 1.01483 | 1538.36 | 1.1027 | –0.293 | 1611 | 25.3 |
| 1337 | 1.06874 | 1422.80 | 1.4207 | 1.082 | 1555 | 35.8 |
| | 1.08112 | 1398.07 | 1.4818 | –1.210 | 1545 | 32.7 |

respect to temperature. These expressions have the following form [27,31,34]:

$$\sigma'(T)_v = \left(\frac{\partial\sigma}{\partial T}\right)_{c,N,f} = -\frac{3k_B R^2\gamma(N,f)}{2\alpha^{2/3}(b+2)r_o^2\, k_n(N,f)^*} F_E\left(\frac{\Theta_E}{T}\right), \quad (22)$$

$$\sigma'(T)_P = \left(\frac{\partial\sigma}{\partial T}\right)_{P,N,f} = \sigma'(T)_v + v\alpha_p\left(\frac{\partial\sigma}{\partial v}\right)_{T,N,f} = \sigma'(T)_v - \frac{2}{3}\sigma\alpha_p\Delta_p. \quad (23)$$

Here, $\alpha_p = (\partial \ln v/\partial T)_P$ is the isobaric thermal volume expansion coefficient, which depends on the nanocrystal size and shape,

$$F_E(y) = \frac{\partial E_w(y)}{\partial(1/y)} = \frac{y^2\exp(y)}{[\exp(y)-1]^2}.$$

Figure 3 shows the behavior of the isochoric and isobaric derivatives of the $\sigma(100)$ function with respect to temperature [in $10^{-6}$ J/(m$^2$ K)]. The upper graphs (a) and (b) are for the function $\sigma'(T)_v = (\partial\sigma/\partial T)_v$, and the lower graphs (c) and (d) are for the function $\sigma'(T)_P = (\partial\sigma/\partial T)_P$. Solid lines are obtained for a macrocrystal (i.e., at $N = \infty$) and dashed lines are obtained for a cubic nanocrystal of $N = 306$ atoms.

Figure 3 shows that at $T = 0$ K the functions $\sigma'(T)_v$ and $\sigma'(T)_P$ reach their maximum at any pressure: $\sigma'(0)_v = \sigma'(0)_P = 0$. At low pressures the inequality is satisfied, $|\sigma'(T)_v| < |\sigma'(T)_P|$. However, at high pressures, this inequality changes to the opposite. Therefore, one cannot equate the functions $\sigma'(T)_v$ and $\sigma'(T)_P$, as some works do. At $T \gg \Theta$, the $\sigma'(T)_v$ function is almost independent of temperature, and the $|\sigma'(T)_P|$ value is greater, the higher the temperature. In the transition to nanocrystal, the magnitude of $|\sigma'(T)_i|$ increases under any $P$-$T$ conditions (here $i = v$ or $P$).

As we indicated in [41], to fulfill the third law of thermodynamics, the $\sigma$ function at $T = 0$ K must satisfy the following conditions:

$$\lim_{T\to 0\ K}\left(\frac{\partial\sigma}{\partial T}\right)_{i,N} = -0,$$

$$\lim_{T\to 0\ K}\left[\frac{\partial(\partial\sigma/\partial T)_{v,N}}{\partial v}\right]_{T,N} = -0,$$

$$\lim_{T\to 0\ K} T\left[\frac{\partial}{\partial T}\left(\frac{\partial\sigma}{\partial T}\right)_{v,N}\right]_{i,N} = -0. \quad (24)$$

The conditions from (24) are valid for any crystal structure, at any specific volume and pressure, as well as for any size and shape of a nanocrystal.

Various methods have been proposed in the literature to calculate the derivative of the $\sigma$ function with respect to temperature for a macrocrystal. However, due to the absence in these works of the state equation taking into account the surface, it remains unclear whether the expression for $\sigma'(T)$ proposed in these works is isochoric or isobaric derivative. Meanwhile, as can be seen from Fig. 3, the difference between the functions $\sigma'(T)_v$ and $\sigma'(T)_P$ is significant, especially when $P = 0$.

In some works, a linear approximation of the following form was used for the isobaric or isochoric temperature dependence of the specific surface energy [42]:

$$\sigma(T) = \sigma(T = 0\ \text{K}) - \text{const}\ T. \quad (25)$$

However, as can be seen from Fig. 3, approximation (25) is valid only at high temperatures: $T \gg \Theta$ (for $i = v$), or at high pressures (for $i = v$ or $i = P$). The use of approximation (25) at low temperatures can lead to both numerical errors and violation of the third law of thermodynamics (24).

## IV. DISCUSSION

Why in some works was the increase of the $\sigma$ function at the isomorphic-isothermal decrease of the nanoparticle size obtained? Let us explain it on the example of Refs. [5,6], taking into account the results obtained by us.

In Ref. [5], a spherical core-shell model for a gold nanocrystal at $T = 0$ K was studied by the method of "combination of atomistic modeling and continuum mechanics." At the same time, the presence of surface pressure was taken into account according to the Laplace formula (which is valid for the liquid phase) only for the shell region. This led to the fact that the shell region turned out to be highly compressed compared to the volume. Consequently, it was found in [5] that both the specific surface energy and the Young's modulus increase with decreasing nanocrystal size. This contradicts the $P(v/v_o)$ dependence for macro- and nanocrystal from Fig. 1, and the results of [36–40], where a decrease in the elastic modulus $B_T$ with decreasing nanocrystal size was obtained. An error of the authors of [5] is also the division of the equilibrium system into two different phases, core and shell, for which different regularities were applied. This violates the conditions of thermodynamic equilibrium and leads to strong gradients of properties over the nanocrystal volume.

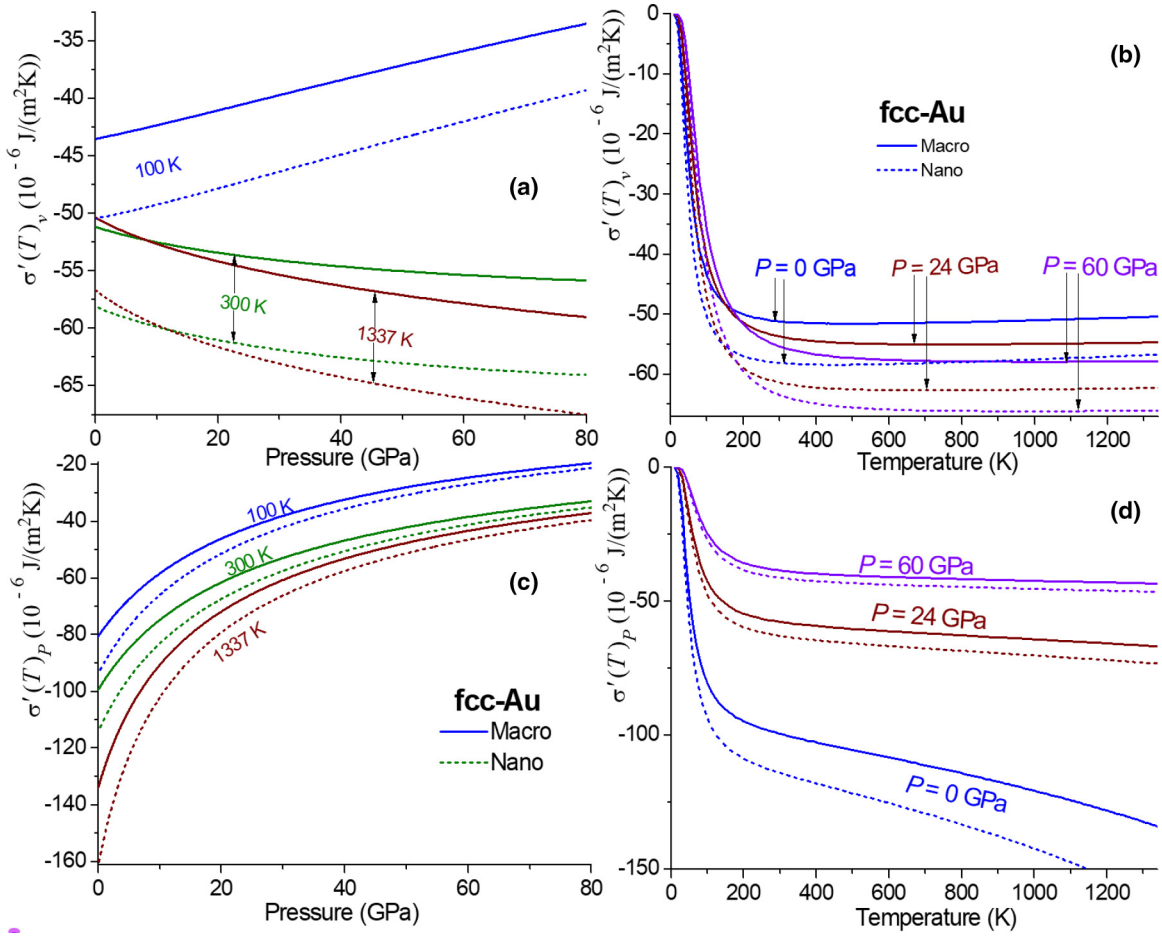


FIG. 3. Behavior of isochoric (upper graphs) and isobaric (lower graphs) derivatives of specific surface energy with respect to temperature for fcc Au. The isotherms of the baric dependence are shown on the left, and the isobars of the temperature dependence are shown on the right. Solid lines were obtained for a macrocrystal (i.e., at $N = \infty$) and dashed lines were obtained for a cubic nanocrystal of $N = 306$ atoms.

The application of the formulas of equilibrium and reversible thermodynamics to such a system is incorrect.

In the computer method that was used in [6] (as well as in other theoretical works, where an increase of the $\sigma$ function was obtained with isomorphic-isothermal decrease of the nanoparticle size), the following formula was used to calculate the specific surface energy [6, Eq. (4)]:

$$\sigma(N) = \frac{E_{\mathrm{NP}}(N) - E_{\mathrm{ref}}(\infty)}{\Sigma}, \tag{26}$$

where $E_{\mathrm{NP}}(N)$ is the internal energy of a nanoparticle of $N$ atoms and $E_{\mathrm{ref}}(\infty)$ is the internal energy of a macrocrystal.

However, a contradiction arises when calculating the $E_{\mathrm{NP}}(N)$ and $E_{\mathrm{ref}}(\infty)$ functions by this method: $E_{\mathrm{ref}}(\infty)$ is calculated for a macrocrystal at $P_{\mathrm{Macro}} = 0$, while the $E_{\mathrm{NP}}(N)$ function is calculated for a nanocrystal at $P_{\mathrm{Nano}} > 0$. This clearly follows from the results of [6], and it is evident from Fig. 1 and Table I. To obtain $P_{\mathrm{Nano}} = 0$, it is necessary that the nanocrystal be stretched, i.e., that the specific volume or the average distance between the centers of the nearest atoms in the nanocrystal must be larger than in the macrocrystal. This was experimentally shown in [36] for a nanodiamond, and in [43] when studying an fcc-ruthenium nanocrystal. This also follows from the fact that the elastic modulus for a nanocrystal is less than that for a macrocrystal at the same temperature.

For the liquid phase at high temperatures, the surface pressure is much larger than for the solid phase at low temperatures. That is why Ref. [6] has obtained the result $\sigma_l(T = 1500\,\mathrm{K}) > \sigma_s(T = 5\,\mathrm{K})$, both for macro- and for nanosystems. For the liquid phase, this result contradicts the results of [44,45], in which methods that are more correct were used to calculate the size dependence of the $\sigma_l$ function.

Unfortunately, in theoretical works, in which the increase of the $\sigma$ function at isomorphic-isothermal size reduction was obtained, the nanosystem state equation was not studied. Therefore, the authors of these works did not notice that an isomorphic-isothermal size reduction led to compression, i.e., to a decrease in the specific volume of the nanoparticle, and, as a consequence, to an increase in the specific surface energy.

## V. CONCLUSIONS

Within the framework of equilibrium and reversible thermodynamics, expressions determining the dependence of specific surface energy $\sigma$ and surface pressure $P_{Sf}$ on the size and shape of a freestanding nanocrystal under different $P$-$T$ conditions were obtained based on the RP model

and the paired Mie–Lennard-Jones interatomic interaction potential. Based on these expressions, the behavior of the $\sigma(P, T, N, f = 1)$ and $P_{Sf}(P, T, N, f = 1)$ functions for fcc Au has been studied. Calculations performed for a macrocrystal and a cube-shaped nanocrystal of 306 atoms have shown that at $P = 0$ the $P_{Sf}(N)$ function lies in the negative region, and the value $|P_{Sf}(N, P = 0)|$ the higher the temperature, or the more the nanocrystal shape deviates from the most energy-optimal shape (for the RP model it is a cube). With a decrease in $N$ at $P = 0$, the $\sigma(N)$ function decreases more noticeably the higher the temperature, or the more the nanocrystal shape deviates from the most energy-optimal shape.

Based on these results, it is shown that the increase in the $\sigma(N)$ function with an isomorphic-isothermal decrease in the nanocrystal size at $P = 0$, which was obtained in some articles, is not completely correct. In such calculation methods, the nanoparticle was compressed by the surface pressure, which increased with decreasing $N$. This led to a corresponding increase in the $\sigma(N)$ function both with an isomorphic-isothermal decrease in size and with an isomeric (i.e., at $N = \text{const}$) increase in the temperature of the nanoparticle.

## ACKNOWLEDGMENTS

The author is grateful to S. P. Kramynin, N. Sh. Gazanova, Z. M. Surkhayeva, and M. M. Gadjiyeva for fruitful discussions and assistance in the work.

[1] W. R. Tyson and W. A. Miller, Surface free energies of solid metals: Estimation from liquid surface tension measurements, Surf. Sci. **62**, 267 (1977).
[2] S. N. Zhevnenko, I. S. Petrov, D. Scheiber, and V. I. Razumovskiy, Surface and segregation energies of Ag based alloys with Ni, Co and Fe: Direct experimental measurement and DFT study, Acta Mater. **205**, 116565 (2021).
[3] D. Vollath, F. D. Fischer, and D. Holec, Surface energy of nanoparticles—influence of particle size and structure, Beilstein J. Nanotechnol. **9**, 2265 (2018).
[4] X. Zhang, W. Li, H. Kou, J. Shao, Y. Deng, X. Zhang, J. Ma, Y. Li, and X. Zhang, Temperature and size dependent surface energy of metallic nano-materials, J. Appl. Phys. **125**, 185105 (2019).
[5] D. Holec, L. Löfler, G. A. Zickler, D. Vollath, and F. D. Fischer, Surface stress of gold nanoparticles revisited, Int. J. Solids Struct. **224**, 111044 (2021).
[6] H. Amara, J. Nelayah, J. Creuze, A. Chmielewski, D. Alloyeau, C. Ricolleau, and B. Legrand, Effect of size on the surface energy of noble metal nanoparticles from analytical and numerical approaches, Phys. Rev. B **105**, 165403 (2022).
[7] E. H. Abdul-Hafidh, Surface free energy and structural transition of tungsten nanosolid, J. Nanopart. Res. **24**, 266 (2022).
[8] R. C. Tolman, The effect of droplet size on surface tension, J. Chem. Phys. **17**, 333 (1949).
[9] K. K. Nanda, Liquid-drop model for the surface energy of nanoparticles, Phys. Lett. A **376**, 1647 (2012).
[10] H. M. Lu and Q. Jiang, Size-dependent surface tension and Tolman's length of droplets, Langmuir **21**, 779 (2005).
[11] S. Xiong, W. Qi, Y. Cheng, B. Huang, M. Wang, and Y. Li, Modeling size effects on the surface free energy of metallic nanoparticles and nanocavities, Phys. Chem. Chem. Phys. **13**, 10648 (2011).
[12] S. Ono and S. Kondo, Molecular theory of surface tension in liquids, *Structure of Liquids* (Springer, Berlin, Heidelberg, 1960), pp. 134–280.
[13] S. S. Rekhviashvili, Size dependence of the surface tension of a small droplet under the assumption of a constant Tolman length: Critical analysis, Colloid J. **82**, 342 (2020).
[14] J. Wang and S. Q. Wang, Surface energy and work function of fcc and bcc crystals: Density functional study, Surf. Sci. **630**, 216 (2014).
[15] S. De Waele, K. Lejaeghere, M. Sluydts, and S. Cottenier, Error estimates for density-functional theory predictions of surface energy and work function, Phys. Rev. B **94**, 235418 (2016).
[16] M. N. Magomedov, On the size dependences of the crystal-liquid phase transition parameters, Tech. Phys. **59**, 675 (2014).
[17] V. D. Nguyen, F. C. Schoemaker, E. M. Blokhuis, and P. Schall, Measurement of the curvature-dependent surface tension in nucleating colloidal liquids, Phys. Rev. Lett. **121** 246102 (2018).
[18] D. Kim, J. Kim, J. Hwang, D. Shin, S. An, and W. Jhe, Direct measurement of curvature-dependent surface tension of an alcohol nanomeniscus, Nanoscale **13**, 6991 (2021).
[19] M. X. Lim, B. VanSaders, A. Souslov, and H. M. Jaeger, Mechanical properties of acoustically levitated granular rafts, Phys. Rev. X **12**, 021017 (2022).
[20] L. D. Landau and E. M. Lifshitz, *Statistical Physics* (Pergamon, Oxford, 1980), Vol. I.
[21] E. A. Moelwyn-Hughes, *Physical Chemistry* (Pergamon, London, 1961).
[22] M. N. Magomedov, Dependence of the surface energy on the size and shape of a nanocrystal, Phys. Solid State **46**, 954 (2004).
[23] M. N. Magomedov, On the statistical thermodynamics of a free-standing nanocrystal: Silicon, Crystallogr. Rep. **62**, 480 (2017).
[24] M. N. Magomedov, On the surface pressure of nanocrystal, Nanotechnol. Russ. **9**, 293 (2014).
[25] M. N. Magomedov, New "surface" criterion of melting, Tech. Phys. **58**, 927 (2013).
[26] E. L. Nagaev, Small metal particles, Sov. Phys. Usp. **35**, 747 (1992).
[27] M. N. Magomedov, Study of properties of fcc-Au-Fe alloys in macro- and nano-crystalline states under various *P-T*-conditions, J. Phys. Chem. Solids **151**, 109905 (2021).
[28] E. N. Ahmedov, Size dependence of molybdenum melting temperature, Phys. B (Amsterdam, Neth.) **571**, 252 (2019).
[29] S. P. Kramynin, Change of baric dependencies of thermophysical properties under variation of the size and shape of niobium nanocrystal, J. Phys. Chem. Solids **143**, 109464 (2020).
[30] S. P. Kramynin, Theoretical study of the size dependencies of the thermodynamic properties of tungsten at various pressures and temperatures, J. Phys. Chem. Solids **152**, 109964 (2021).

[31] M. N. Magomedov, Temperature and pressure dependences of the surface energy for a macro- and nanocrystal, Phys. Solid State **63**, 1595 (2021).

[32] S. P. Kramynin, Theoretical study of concentration and size dependencies of the properties of Mo-W alloy, Solid State Sci. **124**, 106814 (2022).

[33] R. Briggs, F. Coppari, M. G. Gorman, R. F. Smith, S. J. Tracy, A. L. Coleman, A. Fernandez-Panella, M. Millot, J. H. Eggert, and D. E. Fratanduono, Measurement of body-centered cubic gold and melting under shock compression, Phys. Rev. Lett. **123**, 045701 (2019).

[34] M. N. Magomedov, About the gold properties and the approximations used to calculate high-pressure high-temperature properties, Comput. Condens. Matter **31**, e00673 (2022).

[35] M. N. Magomedov, Study of the melting temperature baric dependence for Au, Pt, Nb, Vacuum **213**, 112079 (2023).

[36] M. Mohr, A. Caron, P. Herbeck-Engel, R. Bennewitz, P. Gluche, K. Brühne, and H. -J. Fecht, Young's modulus, fracture strength, and Poisson's ratio of nanocrystalline diamond films, J. Appl. Phys. **116**, 124308 (2014).

[37] A. Rida, E. Rouhaud, A. Makke, M. Micoulaut, and B. Mantisi, Study of the effects of grain size on the mechanical properties of nanocrystalline copper using molecular dynamics simulation with initial realistic samples, Philos. Mag. **97**, 2387 (2017).

[38] M. Goyal and B. R. K. Gupta, Study of shape, size and temperature-dependent elastic properties of nanomaterials, Mod. Phys. Lett. B **33**, 1950310 (2019).

[39] J. Li, B. Lu, H. Zhou, C. Tian, Y. Xian, G. Hu, and R. Xia, Molecular dynamics simulation of mechanical properties of nanocrystalline platinum: Grain-size and temperature effects, Phys. Lett. A **383**, 1922 (2019).

[40] I. M. Padilla Espinosa, T. D. B. Jacobs, and A. Martini, Atomistic simulations of the elastic compression of platinum nanoparticles, Nanoscale Res. Lett. **17**, 96 (2022).

[41] M. N. Magomedov, The temperature dependence of nanocrystal heat capacity, J. Surf. Invest.: X-ray, Synchrotron Neutron Tech. **6**, 86 (2012).

[42] S. Zhu, K. Xie, Q. Lin, and R. Cao, Experimental determination of surface energy for high-energy surface: A review, Adv. Colloid Interface Sci. **315**, 102905 (2023).

[43] M. Zhao and Y. Xia, Crystal-phase and surface-structure engineering of ruthenium nanocrystals, Nat. Rev. Mater. **5**, 440 (2020).

[44] S. W. Cui, J. A. Wei, Q. Li, W. W. Liu, P. Qian, and X. S. Wang, Tolman length of simple droplet: Theoretical study and molecular dynamics simulation, Chin. Phys. B **30**, 016801 (2021).

[45] S. Gong, Z. Hu, L. Dong, and P. Cheng, Temperature- and curvature-dependent surface tensions and Tolman lengths for real fluids: A mesoscopic investigation, Phys. Fluids **35**, 073315 (2023).